Journal of Experimental Pharmacology

Dovepress
Taylor & Francis Group

Open Access Full Text Article

ORIGINAL RESEARCH

Two Novel Compounds Isolated from the Marine Fungal Symbiont of *Aspergillus unguis* Induce Apoptosis and Cell Cycle Arrest in Breast Cancer Cells: In vitro Study

Muhammad Hasan Bashari[1], Mochamad Untung Kurnia Agung[2], Eko Fuji Ariyanto[1], Laode Muhammad Ramadhan Al Muqarrabun[3], Syefira Salsabila[3], Agus Chahyadi[3], Andi Rifki Rosandy[3], Ervi Afifah[4], Merry Afni[5], Harold Eka Atmaja[5], Tenny Putri[5], Fitria Utami[5], Beginer Subhan[6], Syafrizayanti[7], Yosie Andriani[8], Elfahmi[3,9]

[1]Department of Biomedical Sciences, Faculty of Medicine, Universitas Padjadjaran, Bandung, West Java, Indonesia; [2]Department of Marine Science, Faculty of Fisheries and Marine Science, Universitas Padjadjaran, Bandung, West Java, Indonesia; [3]University Center of Excellence for Nutraceuticals, Bioscience and Biotechnology Research Center, Bandung Institute of Technology, Bandung, West Java, Indonesia; [4]Graduate School of Master Program, Faculty of Medicine, Universitas Padjadjaran, Bandung, Indonesia; [5]Biomedical Laboratory, Faculty of Medicine, Universitas Padjadjaran, Bandung, West Java, Indonesia; [6]Department of Marine Science and Technology, Faculty of Fisheries and Marine Science, IPB University, Bogor, West Java, Indonesia; [7]Biochemistry Laboratory, Department of Chemistry, Universitas Andalas, Padang, West Sumatera, Indonesia; [8]Institute of Climate Adaptation and Marine Biotechnology, Universiti Malaysia Terengganu, Kuala Nerus, Terengganu, Malaysia; [9]School of Pharmacy, Bandung Institute of Technology, Bandung, West Java, Indonesia

Correspondence: Muhammad Hasan Bashari, Department of Biomedical Sciences, Faculty of Medicine, Universitas Padjadjaran, Bandung, 40161, West Java, Indonesia, Email bashari@unpad.ac.id; Elfahmi, School of Pharmacy, Bandung Institute of Technology, Bandung, West Java, Indonesia, Email elfahmi@fa.itb.ac.id

Purpose: A promising feature of marine sponges is the potential anticancer efficacy of their secondary metabolites. The objective of this study was to explore the anticancer activities of compounds from the fungal symbiont of *Aaptos suberitoides* on breast cancer cells.

Methods: In the present research, *Aspergillus unguis*, an endophytic fungal strain derived from the marine sponge *A. suberitoides* was successfully isolated and characterized. Subsequently, ethyl acetate extraction and isolation of chemical constituents produced was performed. The structures of the isolated compounds were identified using several spectroscopic methods, ie, UV, NMR, and mass spectrometry. Thereafter, MDA-MB-231, MCF-7 breast cancer cells and HaCat cells were treated with the isolated compounds. Not only viability, apoptosis, and cell cycle analyses were conducted, but also the mRNA expression of *MCL1, BCL2L1, AKT1* and *CDK2* were evaluated.

Results: The extract showed cytotoxic activity in breast cancer cells. Two novel compounds were successfully isolated and identified, ie, Unguisol A (15.1 mg) and Unguisol B (97.9 mg). Both compounds share the same basic skeleton and comprise an aromatic ring which is attached to a sulphur-containing, seven-membered ring via an oxygen atom. This marked the first-time isolation of Unguisol A and Unguisol B from *A. unguis*, highlighting their novelty. Both compounds induced early apoptosis ($p < 0.01$) and cell cycle arrest at the S phase ($p < 0.05$) in MDA-MB-231 cells, but not in HaCat cells. Both compounds suppressed *BCL2L1* and *AKT1* mRNA expression ($p < 0.01$).

Conclusion: Two novel compounds were isolated from *A. unguis*. Unguisol A and Unguisol B induced apoptosis in MDA-MB-231 breast cancer cells via *BCL2L1* mRNA downregulation, while both compounds induced cell cycle arrest at the S phase through *AKT1* mRNA downregulation.

Keywords: *Aspergillus unguis*, drug screening assays, Porifera, triple negative breast neoplasms

Received: 14 October 2024
Accepted: 12 December 2024
Published: 22 January 2025

Graphical Abstract

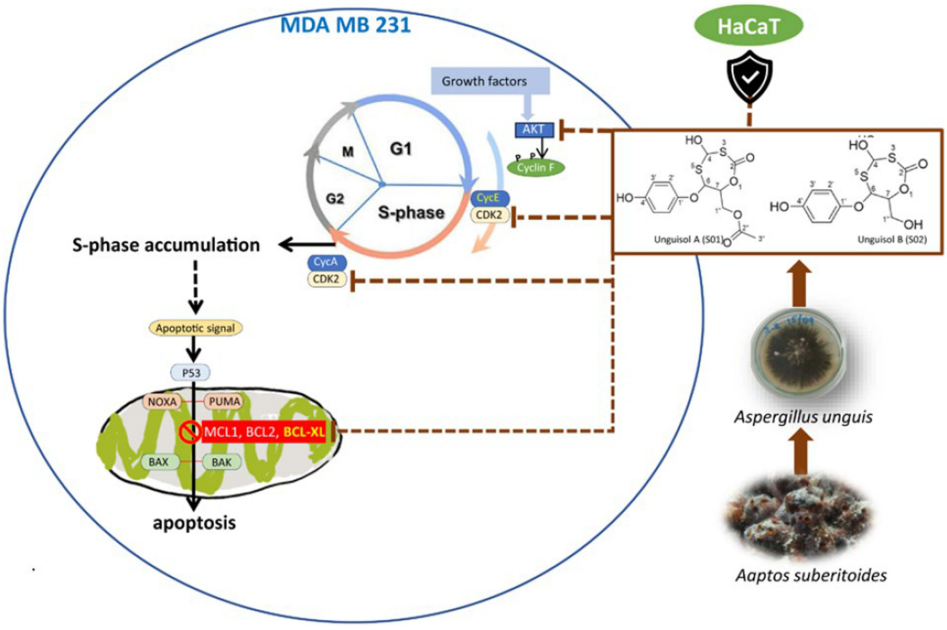

Introduction

Triple negative breast cancer constitutes a specific subtype of breast cancer characterized by the most pronounced clinical presentations, the most unfavorable prognosis, and an aggressive pathological behavior. The significant molecular heterogeneity exhibited by various subtypes of breast cancer, such as luminal A, luminal B, human epidermal growth factor receptor 2-positive, basal type A, basal type B, and claudin-low, presents substantial challenges to the implementation of personalized chemotherapy regimens and culminates in the emergence of resistance to chemotherapeutic agents.[1]

The marine ecosystem constitutes a significant natural asset in the realm of pharmacological exploration. For instance, marine sponges represent a promising reservoir of pharmaceutical compounds. Extensive research on drugs derived from marine organisms has been carried out in the last decade. It has been hypothesized that compounds isolated from such organisms may possess anticancer activity. Our previous data showed that *Stylissa carteri* and *Aaptos suberitoides* are sponges with potential anticancer effects.[2,3] Unfortunately, a limited number of raw materials pose a threat to sponge biodiversity and an obstacle to the compound isolation process. The investigation into the biodiversity and cultural significance of sponges within their indigenous ecosystems represents a pivotal component in the stewardship and sustainable exploitation of marine biological resources. The symbiotic microorganisms associated with sponges serve as a viable source of secondary metabolites.

The interaction between sponge and microorganisms indicates the presence of diversity and symbiotic richness of microorganisms. These organisms are an important source of marine active compounds found mostly in sponges that are primitive metazoans.[4] As microorganisms that are symbiotic with sponges, fungi can produce more active compounds despite their limited abundance versus bacterial symbionts.[5]

Fungi found in sponges live in extreme environments; hence, they utilize certain metabolic pathways to synthesize different metabolic structures.[6] The production of secondary metabolites in fungi derived from sponges depends on the characteristics of the oceanic environment, such as depth, hydrostatic pressure, temperature, sunlight penetration, salt content, and oxygen concentration, as well as the ability of fungi to maintain and compete for habitat space.[6–8]

From 1998 to 2017, research studies on microorganism symbionts in sponges have reported 774 new compounds.[9] As a reservoir of bioactive constituents pertinent to the pharmaceutical domain, it has been evidenced that marine sponges exhibit significant anticancer properties.[10]

Several studies have reported the potential of fungal symbionts as anticancer agents. In this study, an endophytic fungi, *Aspergillus unguis*, was successfully isolated from marine sponge *A. suberitoides* and grown in culture media. The objective of this research was to extract secondary metabolites and examine its anticancer efficacy in vitro.

Materials and Methods

Chemicals and Reagents

Fetal bovine serum (Gibco, Brazil, South America, cat No. 10270106), RPMI 1640 medium (Gibco, New York, USA and Scotland, the UK cat No. 11875093), and penicillin/streptomycin (cat No. 15140122) were obtained from Gibco (New York, USA). Dimethyl sulfoxide (Sigma, Missouri, USA, catalog number D8418) and MTT (Sigma, Missouri, USA, catalog number M2128) were acquired from Sigma–Aldrich (Missouri, USA). The remaining reagents were sourced from Merck (USA). Cisplatin and Paclitaxel were gifted from pharmacy Dr. Hasan Sadikin Hospital, Bandung, Indonesia.

Sampling of Marine Sponge *A. suberitoides*

Marine sponges *A. suberitoides* were collected from the waters of Harapan Island, Seribu Islands (Indonesia), located at 106°34'51.052" E and 5°38'55.462" S. *A. suberitoides* represents one of the predominant sponge species within this particular region.[11] Sponge samples were obtained at a depth of 3–10 m and cut using a knife. Consequently, the specimens were preserved in a sample tube that comprised 10% glycerin, placed within a refrigerated container, and subsequently conveyed to the laboratory.

Isolation, Cultivation, and Identification of Endophytic Fungi *A. unguis*

At the laboratory, the sponge *A. suberitoides* was cleansed under aseptic conditions and was cut (dimensions: approximately 1 cm × 1 cm × 1 cm) using sterile scissors and tweezers. The cut samples were placed in a sterile Petri dish and exposed to 70% alcohol, 5.25% sodium hypochlorite (NaOCl) (Sigma, Missouri, USA), and 70% alcohol (Onemed, Sidomojo, West Java, Indonesia) for 1 min, 5 min, and 30s, respectively; finally, the samples were rinsed with aquadest (Ikapharmindo Putramas, West Jakarta, Indonesia) for 1 min.[12]

Subsequently, the sponge segments that had undergone pre-treatment were positioned on the surface of the Potato Dextrose Agar (PDA) (Oxoid, UK) medium contained within a Petri dish and incubated for a duration of 14 days at ambient temperature. The emerging tips of fungal hyphae from the sponge segments were subjected to multiple rounds of sub-culturing on the identical growth medium to achieve pure fungal colonies. The colonies were subsequently characterized macroscopically based on their color, margin characteristics, and elevation. After staining with lactophenol cotton blue, the characteristics of fungal mycelia were observed under a microscope. All the single fungal isolates were archived at the Laboratory of Microbiology and Molecular Biotechnology, which is situated within the Department of Marine Science, under the Faculty of Fisheries and Marine Science at Universitas Padjadjaran (Bandung, Indonesia).

The genomic deoxyribonucleic acid (gDNA) of endophytic fungi isolates was isolated from 100 mg of fungal mycelium (procured from fungi cultivated in broth medium) utilizing the ZymoBIOMICS DNA/RNA Miniprep kit (Irvine, California, USA). The internal transcribed spacer (ITS) region was amplified through polymerase chain reaction (PCR) employing GoTaq Green PCR Master Mix (Promega, USA) with the subsequent primer pair: ITS5-forward (5′-GGA AGT AAA AGT CGT AAC AGG-3′) and ITS4-reverse (5′-TCC TCC GCT TAT TGA TAT GC-3′).[13,14] The total volume (25 µL) of the PCR reaction contained 2 µL of the extracted fungal genomic DNA, 1.25 µL of each primer, 8 µL of nuclease-free water, and 12.5 µL of GoTaq Green PCR Master Mix. PCR amplification was performed as follows: 2 min at 95 C; 30 cycles at 95°C for 60s, at 55°C for 60s, and at 72°C for 2 min; and a final cycle at 72°C for 5 min. PCR products were subsequently sent to 1st Base Sequencing Service (Malaysia) for sequencing. Thereafter, the nucleotide sequence results were aligned with data from the National Center for Biotechnology Information database using the Basic Local Alignment Search Tool (BLAST) and by using BioEdit and Molecular Evolutionary Genetics Analysis Version 11 (MEGA11). The phylogenetic dendrogram

of fungal isolates was formulated employing the neighbor-joining algorithm, accompanied by a bootstrap analysis consisting of 1,000 iterations.[15] One of the endophytic fungi that we managed to isolate was *A. unguis* and examined further in this research (Supplementary Data and Supplementary Figure 1).

Small-Scale Fermentation and the Collecting of Secondary Metabolites from *A. unguis*

Small-scale fermentation assay was performed according to the protocol established by Kjer et al.[16] In summary, seven to eight mycelial plugs were extracted from the actively proliferating margin of *A. unguis* and subsequently inoculated into 100 mL of PDB (Oxoid, UK). This culture was subjected to incubation at ambient temperature under static and dark conditions for a duration of 30 days. Thereafter, fungal mycelia and supernatant were isolated through centrifugation at 4,000 rpm for five minutes and subsequently filtered utilizing filter paper (Whatman No. 1, Sigma, Clifton, USA). Afterwards, a single extraction of mycelia-free supernatant was carried out with ethyl acetate through liquid–liquid fractionation. The fractions of ethyl acetate were subjected to evaporation under reduced pressure at a temperature of 40°C utilizing a rotary evaporator. The resultant dried crude extracts were preserved at a temperature of −20°C pending subsequent analyses.

Isolation and Purification of Compounds from *A. unguis*

Crude ethyl acetate extract of *A. unguis* (627.5 mg) was re-dissolved in methanol to separate residual salts, yielding 350 mg of salt-free extract. The extract was fractionated using centrifugal chromatography (normal phase) with a gradient solvent containing *n*-hexane-ethyl acetate (7:3, 6:4, and 5:5, volume/volume) to yield nine fractions (A–I). Fraction F was compound 1 (15.1 mg). Fraction C was purified again using the same method to yield compound 2 (97.9 mg).

Spectroscopic Analysis

Spectroscopic analysis of the purified compounds was performed using 1D and 2 D NMR (500 MHz; Bruker), LC-MS /MS TQD (Waters), and HR-MS/MS QTOF (Waters).

Compound **S01**. Yellow oil; $C_{11}H_{12}O_6S_2$; ESIMS− calc. for $[M+OH]^-$ 321.34672. Found 321.02. HR-ESIMS+ calc. for $[M+H_2O+Na]^+$ 345.33968. Found 345.0220; UV-Vis (nm): 277.4; FTIR (cm^{-1}): 3354, 1636; ^{1}H NMR (500 MHz, CD_3OD) δ (ppm): 6.23 (1H, *s*, H-4), 5.16 (1H, *d, J* = 2.5 hz, H-6), 4.14 (1H, *m*, H-7), 7.64 (2H, *d, J* = 8.8 hz, H-2′), 8.19 (2H, *d, J* = 8.8 hz, H-3′), 3.81 (1H, *dd, J* = 10.8, 7.2 hz, H-1"a), 3.61 (1H, *dd, J* = 10.8, 6.1 hz, H-1"b); ^{13}C NMR (125 MHz, CD_3OD) δ (ppm): 166.6 (C-2), 67.4 (C-4), 71.3 (C-6), 58.5 (C-7), 151.6 (C-1'), 128.4 (C-2'), 124.2 (C-3'), 148.6 (C-4'), 62.2 (C-1").

Compound **S02**. Yellow oil; $C_{13}H_{14}O_7S_2$; ESIMS− calc. for $[M+OH]^-$ 363.3834. Found 363.01. HR-ESIMS+ calc. for $[M+H_2O+Na]^+$ 387.3811. Found 386.8518; UV-Vis (nm): 275.1; FTIR (cm^{-1}): 3367, 2506, 1676, 1516, 1345; ^{1}H NMR (500 MHz, CD_3OD) δ (ppm): 6.20 (1H, *s*, H-4), 5.08 (1H, *d, J* = 2.5 hz, H-6), 4.40 (1H, *m*, H-7), 7.65 (2H, *d, J* = 8.8 hz, H-2'), 8.18 (2H, *d, J* = 8.8 hz, H-3'), 4.37 (1H, *dd, J* = 10.8, 5.4 hz, H-1"a), 4.22 (1H, *dd, J* = 10.8, 7.9 hz, H-1"b), 2.03 (1H, *m*, H-3"); ^{13}C NMR (125 MHz, CD_3OD) δ (ppm): 166.7 (C-2), 67.2 (C-4), 71.7 (C-6), 55.7 (C-7), 150.8 (C-1'), 128.4 (C-2'), 124.2 (C-3'), 148.8 (C-4'), 64.8 (C-1"), 172.5 (C-2"), 20.6 (C-3").

Cell Culture and Conditions

MDA-MB-231 cells (TNBC cell line) were obtained from Dr. Thordur Oskarsson (Deutsches Krebsforschungszentrum, DKFZ, Heidelberg, Germany), MCF-7 cells and HCC-1954 cells were from Dr Wiemann (DKFZ), and HaCat cells were obtained from Ahmad Faried, dr., Sp.BS., Ph.D. (Dr. Hasan Sadikin General Hospital, Bandung, Indonesia). MDA-MB -231, HCC-1954, MCF-7 and HaCaT cells were cultured in RPMI 1640 (Gibco, New York, USA and Scotland, the UK cat No. 11875093), medium supplemented with 10% fetal bovine serum (Gibco, Brazil, South America, cat No. 10270106) and 1% penicillin/streptomycin ((cat No. 15140122) were obtained from Gibco (New York, USA) at 37°C with 5% CO_2. This study including utilization of all cell lines used was approved by the Research Ethics Committee of Universitas Padjadjaran (no. 1189/UN6.KEP/EC/2024).

Cytotoxicity Assay

MTT assay was used to evaluate the cytotoxic activity of isolated compounds in breast cancer cells. Cells were seeded in a 96-well plate, incubated for 24 h, and treated with serial concentrations of the compounds for 72 h. Next, the cells were incubated with MTT solution (Sigma, Missouri, USA, cat No. M2128) for 4 h. Dimethyl sulfoxide solution (Sigma, Missouri, USA cat No. D8418) was added to stop the reaction and dissolve the formazan crystal. Finally, the absorbance was recorded at 550 nm wavelength using a Thermo labsystem 352 Multiskan MS microplate reader (Thermo Electron Corporation, Finland). The assay was carried out in triplicate for each culture.

Annexin V Apoptosis Detection

Cells were cultured in RPMI basal medium (Gibco, New York, USA and Scotland, the UK cat No. 11875093) and treated with 75 µg/mL S01 or S02 for 48 h. Subsequently, the cells were washed with phosphate-buffered saline (Gibco, Cat no 70011044, Paisley, the UK) and co-stained with fluorescein isothiocyanate-labeled Annexin V and PI using the Dead Cell Apoptosis Kits with Annexin V for Flow Cytometry (Cat. No.: V13242; Invitrogen, Eugene, US) according to the instructions provided by the manufacturer. Apoptosis was assessed utilizing a FACS Lyric flow cytometer (BD Biosciences). The resultant data were subjected to analysis through the FlowJo_v10.8.1 software (BD; Becton, Dickinson & Company).

Cell Cycle Evaluation

Cells were maintained in the RPMI medium and subsequently subjected to treatment with 75 µg/mL S01 or S02 for a duration of 48 hours. Next, cells were washed with phosphate-buffered saline and fixed with methanol, and the DNA was stained with PI (Cat. No.: P3566; Invitrogen, Eugene, US) according to the instructions provided by the manufacturer. The deoxyribonucleic acid content was quantified utilizing a FACS Lyric flow cytometer (BD Biosciences). The resultant data were subjected to analysis employing the Watson model via the FlowJo_v10.8.1 software (BD). This assay was performed in duplicate.

RNA Extraction

Following the guidelines provided by the manufacturer, RNA extraction was carried out using a Quick RNA Miniprep plus (Zymoresearch, Cat. No R1058). Subsequently, nanodrop spectrophotometry at 260/280 nm was used to quantify the RNA purity and concentration.

mRNA Level Quantification of *MCL1, BCL2L1, AKT1 and CDK2*

Table 1 presents the primer sequences constructed by the IDT primerquest tool using reference sequences from the NCBI database. Among these primers, *ACTB* (beta actin) was utilized to normalize the expression levels of target genes. My Taq One step RTPCR (Bioline, Cat. No BIO-72005) was used for the RT-qPCR mix reaction according to the manufacturer's instructions. Real-time qPCR was performed using a Rotor-Gene Q (Qiagen) with the reverse transcription at temperature 45°C for 10 minutes and then polymerase activation at 95°C for 2 minutes. Next, 40 cycles of denaturation at 95°C for 5 minutes and annealing at 52°C for 10 minutes (this condition was for *MCL1, BCL2L1, AKT1 and CDK2*). The last step was elongation at 72°C for 5 minutes. All data were analyzed from a triplicate of three independent experiments. The mRNA expression was analyzed using the Livak method with the formula $2^{-\Delta\Delta Ct}$.

Table 1 Primer Sequences

Primer	Forward (5′ – 3′)	Reverse (5′ – 3′)	NCBI Reference	Product Length (bp)
ACTB (Beta actin)	TACAATGAGCTGCGTGTG	ACATGATCTGGGTCATCTTC	NM_001101.5	100
BCL2L1	AGGCGGATTTGAATCTCTTTC	TGAGTCTCGTCTCTGGTTAG	NM_138578.3	88
MCL1	TAAACAAAGAGGCTGGGATG	AGCAGCACATTCCTGATG	NM_021960.5	78
AKT1	GTGTACGAGAAGAAGCTCAG	GGTGTGATGGTGATCATCTG	NM_005163.2	107
CDK2	TCTATGCCTGATTACAAGCC	CAGCATTTGCGATAACAAGC	NM_001798.5	108

https://doi.org/10.2147/JEP.S494777

Data and Statistical Analysis

The data acquired in the present investigation were subjected to evaluations for normality and homogeneity. A one-way analysis of variance (ANOVA), in conjunction with Dunnett's multiple comparison test, was executed to determine significant differences concerning treatment in comparison to the control group. In instances where the assumptions underlying ANOVA were not fulfilled, Kruskal–Wallis non-parametric tests were employed. A minimum of three independent experiments were executed for most of the assays. P-values less than 0.05 were indicative of statistically significant differences. The findings are articulated as the mean ± standard error of the mean. The IC_{50} was ascertained via four-parameter logistic regression analysis. All statistical evaluations were performed utilizing the GraphPad Prism version 9 software (GraphPad Software, La Jolla, CA, USA).

Results

Inhibition of the Viability of MDA-MB-231 Cells and HaCaT Cells by Endophytic Fungi *A. unguis* Extracts Derived from Marine Sponge *A. suberitoides*

Next, the cytotoxicity of *A. unguis* extract on the MDA-MB-231 triple-negative breast cancer (TNBC) cells was subjected to evaluation. Furthermore, HaCaT cells were employed to ascertain the effects of the extracts on normal cellular structures. The results indicated that the extract of *A. unguis* demonstrated a more pronounced cytotoxic effect on TNBC cells in comparison to HaCaT cells (Figure 1). These results indicate that the extract derived from *A. unguis* may possess bioactive compounds that hold the potential for specifically targeting TNBC cells. Consequently, there is promise in further exploration and identification of these bioactive compounds present in the extract.

Identification of Compounds from *A. unguis* Extract

The nuclear magnetic resonance (NMR) spectral data pertaining to both ^{13}C and ^{1}H of compound S01 (Table 2) elucidated the existence of nine carbon signals and seven proton signals. A carbon atom at 166.6 ppm (C-2) indicated

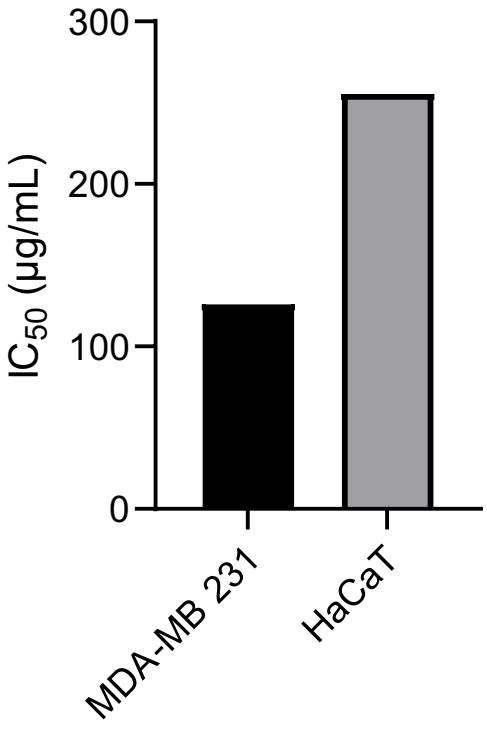

Figure 1 Cytotoxicity of *A. unguis* extract on TNBC and normal cells. MDA-MB-231 and HaCaT cells were exposed to *A. unguis* extract for 72 hours before the MTT assay was conducted. Data represented the average of triplicate measurements from three independent experiments.
Abbreviation: MTT, 3-[4,5-dimethylthiazol-2-yl]-2,5 diphenyl tetrazolium bromide.

Table 2 ^{13}C and ^{1}H NMR Data of Compound S01

No.	δC	Type	δH, mult., (J in Hz), ΣH	COSY	HMBC
1	166.6	C	–		
2	151.6	C	–		
3	148.6	C	–		
4	128.4 (2)	CH	7.64 (d; 8.8 hz; 2H)	H-5	C-3, C-5, and C-6
5	124.2 (2)	CH	8.19 (d; 8.8 hz; 2H)	H-4	C-2
6	71.3	CH	5.16 (d; 2.5 hz; 1H)	H-4, H-5, and H-9	C-2, C-4, C-8, C-9
7	67.4	CH	6.23 (s; 1H)	-	C-1
8	62.2	CH2	3.81 (dd; 10.8, 7.2 hz; 1H)		C-6, C-9
			3.61 (dd; 10.8, 6.1 hz; 1H)		
9	58.5	CH	4.14 (m; 1H)	H-6, H-8	C-1, C-8

Abbreviations: COSY, correlation spectroscopy; HMBC, heteronuclear multiple bond correlation; NMR, nuclear magnetic resonance.

a carbonyl group, which is typical for an ester. Two CH signals at 128.4 (C-2') and 128.2 (C-3') ppm represent two symmetrical olefinic carbon atoms each. These were indicated by the signal intensity, which was significantly higher compared with that of other signals. The presence of two oxygen-attaching carbon signals at 148.6 (C-1') and 151.6 (C-4') ppm signified that the compound contains an aromatic ring. Carbons C-2' and C-3' bound two symmetrical protons each (H-2' and H-3', respectively) with J = 8.8 hz, indicating ortho positions between the two proton signals. The O atom attached to C-1' is directly connected to C-6 (71.3 ppm), which binds to a highly-deshielded doublet proton H-6 (5.16 ppm). The unusually-high chemical shift of H-6 indicated that the proton was attached to more than one electronegative atom. In this case, H-6 was attached to O and S atoms. Similarly, carbon C-4 at 67.4 ppm also binds to a highly-deshielded singlet proton H-4 (6.23 ppm). This phenomenon occurs if the carbon (C-4) is attached to one O atom and two S atoms. The presence of two S atoms next to C-4 caused the high chemical shift of H-4, while C-4 exhibited a chemical shift typical to oxygen-attaching carbon. Proton H-6 was in a neighboring position with multiplet H-7 (4.14 ppm), which was bound to oxygen-binding C-7 (58.5 ppm). Carbon C-1" (62.2 ppm) is also an oxygen-attaching methylene which covalently binds two chemically inequivalent double doublet protons. Of the five non-carbonyl O atoms in the structure, three were hydroxyl groups.

The HRESI-MS analysis showed that the *m/z* value of the singly-charged ion of compound S01 was 345.0220 corresponding to $[M+H_2O+Na]^+$. An additional experiment using LC-ESI-MS/MS TQD generated ion mass of m/z 321.02, which attributed to $[M+OH]^-$ ion. This confirmed the molecular formula of $C_{11}H_{12}O_6S_2$ (calc. MW = 304.33938), 4-hydroxy-7-(hydroxymethyl)-6-(4-hydroxyphenoxy)-1,3,5-oxadithiepan-2-one (Figure 2). The calculation

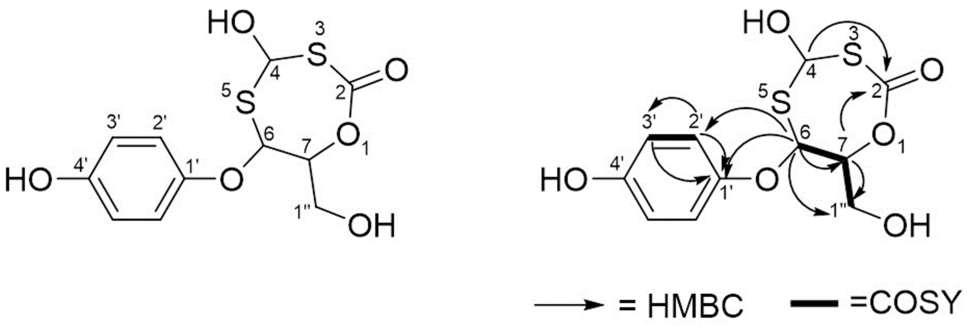

Figure 2 Compound S01 (Unguisol A) Structure and 2D NMR Correlations.

https://doi.org/10.2147/JEP.S494777

Table 3 ^{13}C and ^{1}H NMR Data of Compound S02

No.	δ_C	Type	δH, mult., (J in Hz), ΣH	COSY	HMBC
1	172.5	C	–		
2	166.7	C	–		
3	150.8	C	–		
4	148.8	C	–		
5	128.4 (2)	CH	7.65 (d; 8.8 hz; 2H)	H-6, H-7	C-4, C-7
6	124.2 (2)	CH	8.18 (d; 8.8 hz; 2H)	H-5	C-3, C-4
7	71.7	CH	5.08 (d; 2.5 hz; 1H)	H-5, H-10	C-3, C-5, and C-9
8	67.2	CH	6.20 (s; 1H)		C-2
9	64.8	CH_2	4.37 (dd; 10.8, 5.4 hz; 1H)	H-10	C-1, C-7
			4.22 (dd; 10.8, 7.9 hz; 1H)		C-1, C-10
10	55.7	CH	4.40 (m; 1H)	H-7, H-9	C-2
11	20.6	CH_3	2.03 (s; 3H)		C-1

Abbreviations: COSY, correlation spectroscopy; HMBC, heteronuclear multiple bond correlation; NMR, nuclear magnetic resonance.

of the index of hydrogen deficiency (IHD) was consistent with the molecular formula (IHD = 6), revealing the presence of four π bonds and two rings in the compound structure. 2D NMR experiments (HMBC and COSY) confirmed the positions of carbons and protons (Figure 2), establishing compound S01 to be a newly-reported compound which is named Unguisol A. (Supplementary Figures 2–6)

NMR spectral data of compound S02 (Table 3) showed strikingly similar features to those of S01. The only difference was the presence of an additional carbonyl carbon and a methyl signal at 172.5 (C-2") and 20.6 (C-3") ppm, respectively. The two signals represent an acetyl ester which was attached to a methylene C-1" (64.8 ppm). This acetyl group replaced the hydroxyl group, which was present in compound S01. The HRESI-MS spectral data showed ion mass of 386.8518 established for $[M+H_2O+Na]^+$, establishing molecular formula of $C_{13}H_{14}O_7S_2$ (calc. MW = 346.47606), [4-hydroxy-6-(4-hydroxyphenoxy)-2-oxo-1,3,5-oxadithiepan-7-yl] methyl acetate. This is supported by LC-ESI-MS/MS TQD analysis which gave ion mass of m/z 321.02 corresponding to $[M+OH]^-$ ion. The molecular structure and 2D correlations of compound S02 are depicted in Figure 3. Similar to compound S01, compound S02 is a newly-reported compound and is named Unguisol B. (Supplementary Figures 7–11)

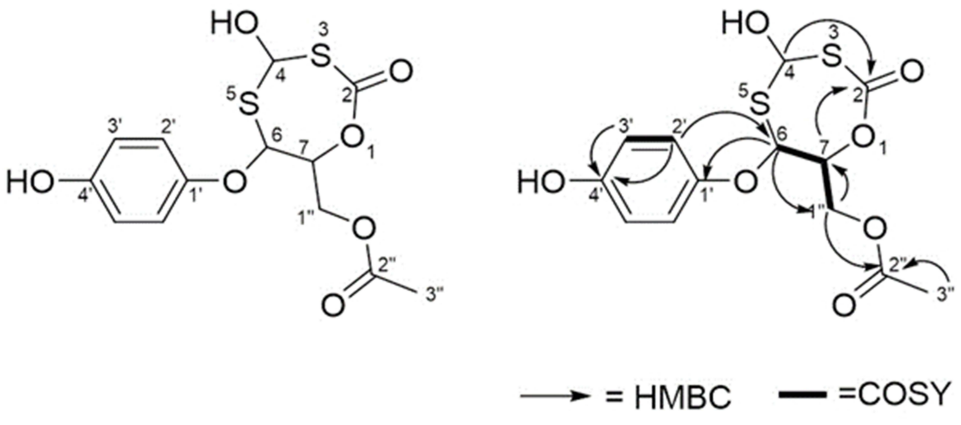

Figure 3 Compound S02 (Unguisol B) Structure and 2D NMR Correlations.

Cytotoxic Effects of Compounds Unguisol A (S01) and Unguisol B (S02) on Breast Cancer Cells

The cytotoxicity of compounds Unguisol A (S01) and Unguisol B (S02) was evaluated using MDA-MB-231 TNBC cells and HCC-1954 HER2+ cells. The cells were exposed to S01 and S02 for 72 h; subsequently, the MTT assay was conducted. The data showed that compound S01 had weak cytotoxic activity in MDA-MB-231 TNBC cells. Surprisingly, the HCC-1954 cells grew further upon exposure to compound S01 (Figure 4A and B). Compound S02 showed cytotoxic activity in both types of cells; the highest activity was observed against MDA-MB-231 cells. These data indicated promising selective activity of this S01 in TNBC cells (Figure 4). The half-maximal inhibitory concentration (IC_{50}) of the S02 compound, ascertainable solely in MDA-MB-231 cells, was recorded at 138.7 μM ($R^2 = 0.9483$).

Compounds Induced Apoptosis Cells Together with Suppression of mRNA of *BCL2L1*, but Not *MCL1* in MDA-MB-231 Cells

Subsequently, the annexin V/propidium iodide (Catalog No.: V13242; Invitrogen, Eugene, US) apoptosis assay was employed to ascertain whether the two compounds elicited apoptotic processes in TNBC cells. MDA-MB-231 cells underwent a treatment duration of 48 hours with concentrations of 75 μg/mL of S01 or S02, which correspond to molar concentrations of 246.43 μM and 216.46 μM, respectively. In addition, the cells were treated with cisplatin as positive control. Moreover, HaCaT cells were also treated with S01 or S02 to represent normal cells. As expected, similar to cisplatin, S01 or S02 treatment induced apoptosis in MDA-MB-231 cells (Figure 5A). The proportion of early apoptotic cells was significantly increased after treatment ($p < 0.01$) (Figure 5B). Importantly, S01 or S02 treatment did not induced apoptosis in HaCaT cells (Figure 5C). The proportion of apoptotic cells did not significantly change after treatment (Figure 5D). Interestingly, cell apoptotic induction of S01 did not prominently occur in MCF-7 cells, a represented cell line of luminal A breast cancer subtype (Supplementary Figure 12 A–C).

The BCL2 family members regulate apoptosis; therefore, anti-apoptosis *MCL1* and *BCL2L1* (*BCL-XL*) mRNA expressions were evaluated. MDA-MB-231 cells were treated for 48 h with 75 μg/mL S01 or S02. The data showed that there was a trend of *MCL1* mRNA expression upregulation upon treatment though statistically not significant ($p > 0.05$) (Figure 5E). Interestingly, *BCL2L1* mRNA expression was suppressed ($p < 0.01$) upon treatment of both compounds (Figure 5F).

Both Compounds Inhibited Cell Cycle and Suppress mRNA Expression of *AKT1* in MDA-MB-231 Cells

Next, cell cycle analysis using PI was performed to examine whether the compounds inhibit proliferation in TNBC cells. MDA-MB-231 cells were treated for 48 h with 75 μg/mL S01 or S02. In addition, the cells were treated with paclitaxel 1nM as positive control. Moreover, HaCaT cells were also treated with S01 or S02 to compare their selectivity effect on normal cells. The data showed that both compounds increased the proportion of cells in the S phase. This finding

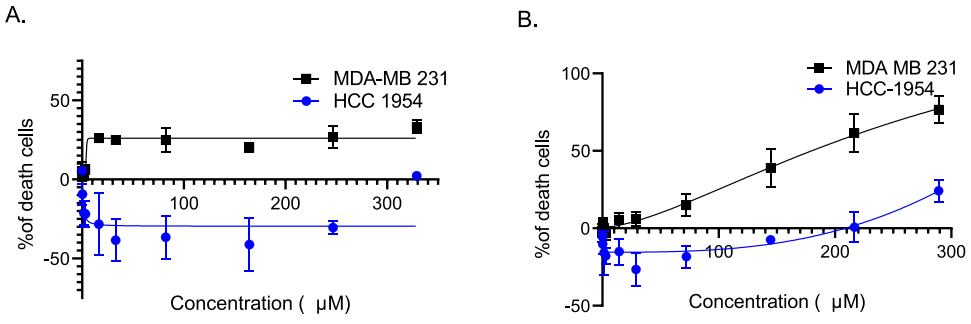

Figure 4 Compound S02 triggered death in MDA-MB-231 cells more potently and selectively than compound S01. MDA-MB-231 and HCC-1954 cells were exposed to compounds S01 (**A**) and S02 (**B**) for 72 hours before the MTT assay was conducted. Data represented the average of triplicate measurements from three independent experiments.

Abbreviation: MTT, 3-[4,5-dimethylthiazol-2-yl]-2,5 diphenyl tetrazolium bromide.

https://doi.org/10.2147/JEP.S494777

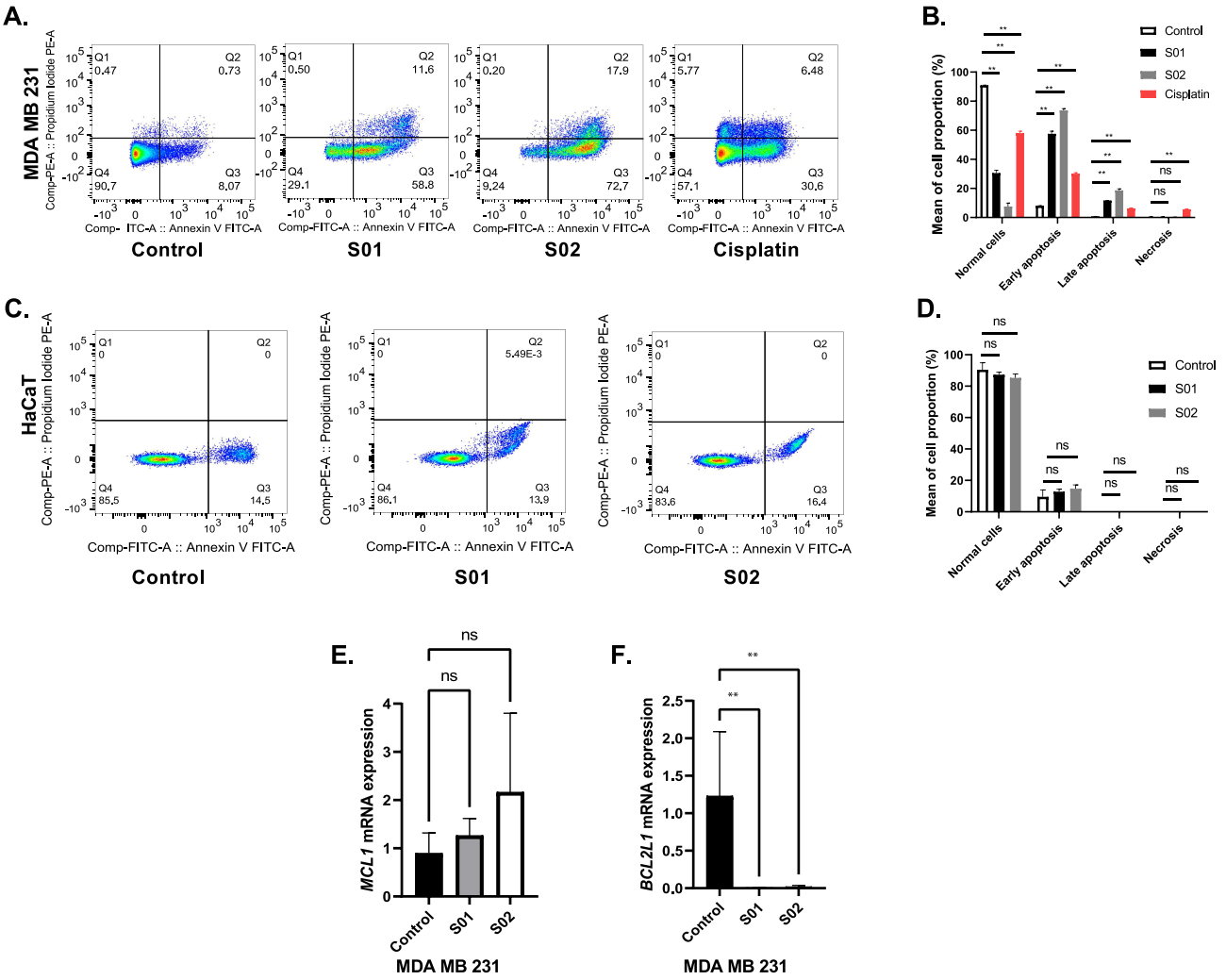

Figure 5 MDA-MB-231 cells were induced apoptosis and suppressed mRNA expression of *BCL2L1* but not *MCL1*. MDA-MB-231 cells and HaCaT cells were exposed to DMSO as control, compound S01, and S02 or cisplatin 30nM for 48 hours before Annexin V/PI staining (**A** and **C**) as well as mRNA isolation were conducted. Data (**B** and **D**) represented the average of duplicate measurements from two independent experiments. *MCL1* (**E**) and *BCL2L1* (**F**) mRNA expression represented the fold average of triplicate measurements from three independent experiments. *, $p < 0.05$; **, $p < 0.01$.
Abbreviations: DMSO, dimethyl sulfoxide; FITC, fluorescein isothiocyanate; ns, not significant; PE, Phycoerythrin.

suggested that both S01 and S02 triggered cell cycle arrest at the S phase (Figure 6A). The proportion of cells in the S phase was significantly increased upon treatment with S01 or S02 ($p < 0.05$ and $p < 0.01$, respectively) (Figure 6B). Consistently, paclitaxel triggered cell cycle arrest at the M phase (Figure 6A and B). Importantly, S01 or S02 treatment did not trigger cell cycle arrest at the S phase in HaCaT cells (Figure 6A and B) nor S01 for MCF-7 cells (Supplementary Figure 12 D–F).

Next, *AKT1, CDK2*, regulator of this S-phase, was evaluated. MDA-MB-231 cells were treated for 48 h with 75 µg/mL S01 or S02. The data showed that there was a trend of suppression of *AKT1* and *CDK2* mRNA expression. This suppression was significant in *AKT1* mRNA (Figure 6C) but not *CDK2* mRNA (Figure 6D).

Discussion

Various studies have emphasized the crucial role played by sponge symbionts, specifically fungi, microbes, and actinomycetes, in the synthesis of a wide range of secondary metabolites exhibiting diverse biological properties.[9] Fungi, in particular, have been identified as producers of a greater variety of bioactive substances in comparison to microbes, owing to their defense mechanisms and competition for living space.[17,18] The abundance of these bioactive

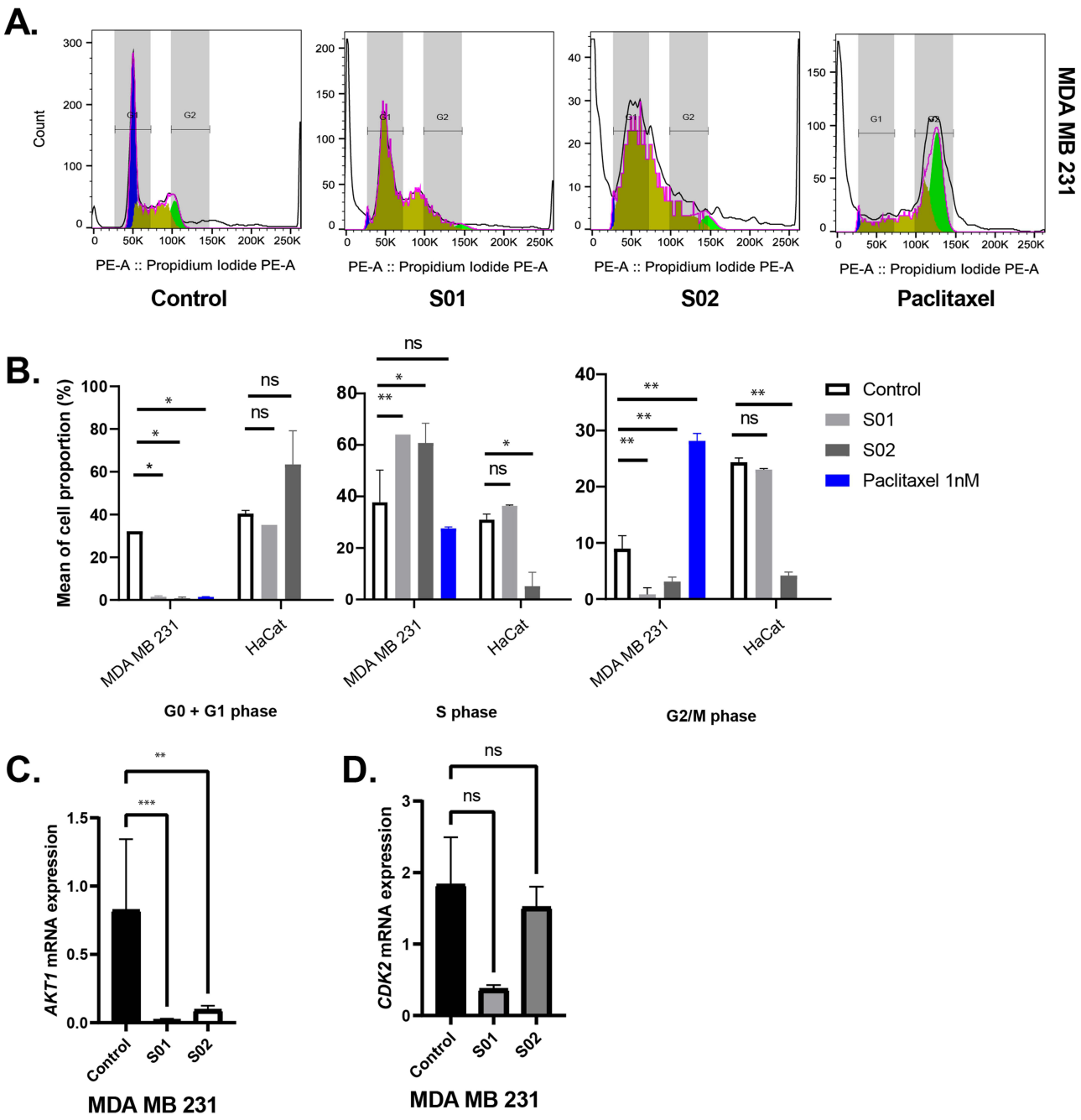

Figure 6 Both compounds S01 and S02 induced cell cycle arrest at the S phase and suppressed mRNA expression of *AKT1* but not *CDK2* in MDA-MB-231 cells. MDA-MB -231 cells and HaCaT cell were exposed to DMSO as control, compound S01, and S02 for 48 h before conducting cell cycle analysis (**A**) and mRNA isolation (**C** and **D**) followed by RT qPCR. Paclitaxel 1nM were used as positive control. Data (**B**) represented the average of duplicate measurements from two independent experiments. *AKT1* (**C**) and *CDK2* (**D**) mRNA expression represented the fold average of triplicate measurements from three independent experiments. *, $p < 0.05$; **, $p < 0.01$, ***, $p < 0.001$. **Abbreviations**: DMSO, dimethyl sulfoxide; ns, not significant.

compounds highlights the significance of fungal symbionts as valuable reservoirs of anticancer agents, supported by multiple scientific investigations.[19]

In this study, we isolated *A. unguis* from marine sponge *A. suberitoides* (Supplementary Figure 1A). These genera are fungal endosymbiont often successfully isolated from marine sponges.[20,21] The extracts from both supernatants were more toxic to cancer cells versus normal cells (Figure 1). Other studies showed >90 compounds isolated from *A. unguis* have demonstrated potential larvicidal, antimicrobial, anticancer, animal growth promotive, antimalarial, and antioxidant

https://doi.org/10.2147/JEP.S494777

activities.[22] Compounds derived from *A. unguis* have undergone comprehensive evaluation against multiple tumor cell lines, with certain compounds exhibiting robust cytotoxic effects on cancer cells.[22]

Aspergillus is a unique source of peptides. Unguisin is a cyclic heptapeptide produced by *A. unguis*.[23,24] The chemical entities identified in *A. unguis* can be categorized into multiple classifications, specifically depsidones, phthalides, cyclopeptides, indanones, diaryl ethers, pyrones, and benzoic acid.[22] Depsides increase the activity of caspase 3 and reactive oxygen species generation and inhibit proto-oncogenic tyrosine kinase.[25] Depsidones consist of depsides, such as ether and cyclic ether; these compounds have anti-tumor activity against MDA-MB-231 cells.[26,27] Another investigation indicated that *A. unguis*, which was isolated from marine sponges in Thailand, exhibited an IC50 value of 0.74 µM. Furthermore, it demonstrated a deleterious effect on MOLT-3 cancer cell lines, characterized by an IC50 of 8.8 µM. Nevertheless, the cytotoxic efficacy against four distinct cellular lineages (namely, HuCCA-1, HepG2, A549, and MOLT-3) remained comparatively low.[28] In this study, two new compounds (S01 and S02) were isolated from the extract of *A. unguis*. Interestingly, compound S02 exhibited a stronger inhibitory effect on the viability of MDA-MB-231 cells than S01 (Figure 4). As expected, both S01 and S02 induced apoptosis in MDA-MB-231 cells but not in HaCaT cells (Figure 5A–5D). Interestingly, the induction of apoptosis by S01 was not notably observed in MCF-7 cells, a representative cell line of the luminal A breast cancer subtype (Supplementary Figure 12 A–C), indicating its specific effect on MDA-MB-231 cells.

The complex mechanism of apoptosis occurring in breast cancer cells is significantly influenced by the nuanced equilibrium between the anti-apoptotic and pro-apoptotic constituents of the BCL-2 protein family.[29,30] MCL-1, a protein characterized by its anti-apoptotic properties, is frequently observed at elevated concentrations in breast carcinoma, thereby serving as an essential function in facilitating cellular viability and conferring resistance against chemotherapeutic agents.[31–33] The increase in *MCL1* mRNA expression following exposure to S02 indicates a strategic response by cancer cells to avoid apoptosis, as MCL-1 functions to counteract apoptotic triggers such as Bim, thereby supporting cell survival. Conversely, the decrease in *BCL2L1* (*BCL-XL*) mRNA expression signals a disturbance in the equilibrium of BCL-2 family proteins, potentially rendering MDA MB 231 cells more susceptible to apoptotic signals.[34] BCL-XL, another anti-apoptotic protein, is also linked to resistance to chemotherapy and cell survival, and reducing its mRNA levels could enhance the apoptotic impact of both S01 and S02.

Furthermore, our data indicated that both substances S01 and S02 induced a halt in the cell cycle at the S phase (Figure 6A and B). There was a notable rise in the percentage of cells in the S phase following exposure to either S01 or S02 ($p < 0.01$ and $p < 0.05$, respectively) (Figure 6B).

Furthermore, in humans, cyclin-dependent kinase 2 (CDK2)–cyclin E (CCNE), CDK1–CCNA, and CDK2–CCNA regulate this S-phase.[35,36] The inquiry concerns the assessment of the impacts of compounds S01 and S02 on the cell cycle, with a specific focus on the S-phase (Figure 6B) and the modulation of *AKT1* and *CDK2* mRNA expression (Figure 6C and D) in MDA-MB-231 cells. The data suggest that exposure to 75 µg/mL of either compound for 48 hours led to a notable inhibition of *AKT1* mRNA expression, while the decrease in *CDK2* mRNA expression was not deemed significant. This finding is in accordance with results from diverse studies on analogous compounds and their modes of operation. For instance, ursolic acid (UA) has demonstrated the capability to induce cell cycle arrest at various phases, including the S-phase, within MDA-MB-231 cells, and significantly reduces essential markers associated with the epithelial–mesenchymal transition (EMT), which is a process vital for the metastasis of cancer.[37] The phosphorylation of CDK2 by Akt constitutes a pivotal element in the complex regulation of the cellular cycle, exerting influence over both its advancement and the initiation of programmed cellular demise referred to as apoptosis. This post-translational modification mediated by Akt exerts a dual effect on CDK2, modulating its activity in a manner that impacts the delicate balance between cell division and cell survival, ultimately shaping the fate of the cell.[36] Further investigation is required in order to delve deeper into the intricacies of the protein level as it pertains to the assessment and analysis of the intricate mechanisms involved in apoptosis and the subsequent arrest of the cell cycle specifically during the S-phase.

While this study provides valuable insights into the apoptotic effects of S01 and S02, several limitations must be acknowledged. The precise mechanisms underlying the observed apoptotic effects have yet to be fully elucidated. Future research will aim to explore these mechanisms in greater depth, particularly through assays assessing the protein levels of key apoptosis and cell cycle-regulated proteins. Additionally, although the study focused primarily on the MDA-MB-231

breast cancer cell line and included HaCaT cells for normal cell selectivity testing, a broader panel of cancerous and non-cancerous cell lines would offer a more comprehensive evaluation of the selectivity and relevance of these compounds across diverse cellular contexts. Finally, to enhance our understanding of the molecular actions of S01 and S02, we recommend conducting molecular modeling studies to identify their specific targets and binding sites. Such studies would contribute to the design of more potent and selective agents in future investigations.

Conclusion

In conclusion, two novel compounds were isolated from *A. unguis*. Unguisol A (S01) and Unguisol B (S02) induced apoptosis in MDA-MB-231 breast cancer cells but not in normal cells via *BCL2L1* mRNA downregulation. In addition, both compounds induced cell cycle arrest at the S phase through *AKT1* mRNA downregulation. The discovery of these two new compounds has opened opportunities for further research on their promising biological activities, particularly anticancer properties.

Institutional Review Board Statement

This study, including utilization of all cell lines used in this study, was approved by the Research Ethics Committee of Universitas Padjadjaran (no. 1189/UN6.KEP/EC/2024).

Acknowledgments

We convey our sincere appreciation to *Balai Taman Nasional Kepulauan Seribu* for granting us the opportunity to collect samples. We thank Fathul Huda, MD, PhD and Putri Halleyana Adrikni Rahman for supporting this project.

Funding

This study was funded by Riset Kolaborasi Indonesia 2022 and by Ministry of Education, Culture, Research, and Technology, Indonesia (No.3018/UN6.3.1/PT.00/2023). The APC was funded by Universitas Padjadjaran.

Disclosure

The authors report no conflicts of interest in this work.

References

1. Palma G, Frasci G, Chirico A, et al. Triple negative breast cancer: looking for the missing link between biology and treatments. *Oncotarget*. 2015;6 (29):26560–26574. doi:10.18632/oncotarget.5306
2. Achmad A, Lestari S, Holik HA, et al. Highly specific L-type amino acid transporter 1 inhibition by JPH203 as a potential pan-cancer treatment. *Processes*. 2021;9(7):1170. doi:10.3390/pr9071170
3. Bashari MH, Huda F, Tartila TS, et al. Bioactive compounds in the ethanol extract of marine Sponge Stylissa carteri demonstrates potential anti-cancer activity in breast cancer cells. *Asian Pacific J Cancer Prev*. 2019;20(4):1199–1206. doi:10.31557/APJCP.2019.20.4.1199
4. Cheng -M-M, Tang X-L, Sun Y-T, et al. Biological and chemical diversity of marine sponge-derived microorganisms over the last two decades from 1998 to 2017. *Molecules*. 2020;25(4):853. doi:10.3390/molecules25040853
5. Vasanthabharathi V. Bioactive potential of symbiotic bacteria and fungi from marine sponges. *African J Biotechnol*. 2012;11(29). doi:10.5897/AJB11.1378
6. Yang Q, Zhang W, Franco CMM. Response of Sponge microbiomes to environmental variations. In: *Symbiotic Microbiomes of Coral Reefs Sponges and Corals*. Springer Netherlands; 2019:181–247. doi:10.1007/978-94-024-1612-1_11
7. Gloer JB. The chemistry of fungal antagonism and defense. *Can J Bot*. 1995;73(S1):1265–1274. doi:10.1139/b95-387
8. Tianero MD, Balaich JN, Donia MS. Localized production of defence chemicals by intracellular symbionts of Haliclona sponges. *Nat Microbiol*. 2019;4(7):1149–1159. doi:10.1038/s41564-019-0415-8
9. Li P, Lu HB, Zhang Y, et al. The natural products discovered in marine sponge-associated microorganisms: structures, activities, and mining strategy. *Front Mar Sci*. 2023:10. doi:10.3389/fmars.2023.1191858
10. Calcabrini C, Catanzaro E, Bishayee A, Turrini E, Fimognari C. Marine sponge natural products with anticancer potential: an updated review. *Marine Drugs*. 2017;15:310. doi:10.3390/md15100310
11. Prabowo B, Fahlevy K, Subhan B, et al. Variation in species diversity and abundance of sponge communities near the human settlement and their bioprospect in Pramuka Island, Jakarta, Indonesia. *AACL Bioflux*. 2023;16(3):1186–1198.
12. Handayani D, Aminah I. Antibacterial and cytotoxic activities of ethyl acetate extract of symbiotic fungi from West Sumatra marine sponge Acanthrongylophora ingens. *J Appl Pharm Sci*. 2017;7(2):237–240. doi:10.7324/JAPS.2017.70234
13. White TJ, Bruns T, Lee S, Taylor J. Amplification and direct sequencing of fungal ribosomal RNA genes for phylogenetics. *PCR Protocols*. 1990;315–322. doi:10.1016/b978-0-12-372180-8.50042-1

14. Raja HA, Miller AN, Pearce CJ, Oberlies NH. Fungal identification using molecular tools: a primer for the natural products research community. *J Nat Prod*. 2017;80(3):756–770. doi:10.1021/ACS.JNATPROD.6B01085/ASSET/IMAGES/LARGE/NP-2016-01085V_0007.JPEG
15. Hall BG. Building phylogenetic trees from molecular data with MEGA. *Mol Biol Evol*. 2013;30(5):1229–1235. doi:10.1093/MOLBEV/MST012
16. Kjer J, Debbab A, Aly AH, Proksch P. Methods for isolation of marine-derived endophytic fungi and their bioactive secondary products. *Nat Protoc*. 2010;5(3):479–490. doi:10.1038/nprot.2009.233
17. Tanod WA, Muliadin, Adel YS, Dewanto DK. Potential marine-derived fungi isolated from sponge in produce new and beneficial compounds. *KAUDERNI J Fish Mar Aquat Sci*. 2020;2(1):52–66. doi:10.47384/kauderni.v2i1.30
18. Alam B, Lǐ J, Gě Q, et al. Endophytic fungi: from symbiosis to secondary metabolite communications or vice versa? *Front Plant Sci*. 2021;12:3060. doi:10.3389/fpls.2021.791033
19. Venkataraman V, Vaithi K, Singaram J. Bioactive novel natural products from marine sponge: associated fungi. *Fungal Reproduction and Growth*. 2022. doi:10.5772/intechopen.101403
20. Sabdaningsih A, Liu Y, Mettal U, et al. A new citrinin derivative from the Indonesian marine sponge-associated fungus Penicillium citrinum. *Mar Drugs*. 2020;18(4):227. doi:10.3390/md18040227
21. Ding B, Yin Y, Zhang F, Li Z. Recovery and phylogenetic diversity of culturable fungi associated with marine sponges Clathrina luteoculcitella and Holoxea sp. in the South China Sea. *Mar Biotechnol*. 2011;13(4):713–721. doi:10.1007/s10126-010-9333-8
22. Domingos LTS, Martins RDS, Lima LM, Ghizelini AM, Ferreira-Pereira A, Cotinguiba F. Secondary metabolites diversity of Aspergillus unguis and their bioactivities: a potential target to be explored. *Biomolecules*. 2022;12(12):1820. doi:10.3390/biom12121820
23. Li W, Jiao F-W, Wang J-Q, et al. Unguisin G, a new kynurenine-containing cyclic heptapeptide from the sponge-associated fungus Aspergillus candidus NF2412. *Tetrahedron Lett*. 2020;61(40):152322. doi:10.1016/j.tetlet.2020.152322
24. Malmstrøm J. Unguisins A and B: new cyclic peptides from the marine-derived fungus Emericella unguis. *J Nat Prod*. 1999;62(5):787–789. doi:10.1021/np980539z
25. Russo A, Piovano M, Lombardo L, Garbarino J, Cardile V. Lichen metabolites prevent UV light and nitric oxide-mediated plasmid DNA damage and induce apoptosis in human melanoma cells. *Life Sci*. 2008;83(13–14):468–474. doi:10.1016/j.lfs.2008.07.012
26. Ebrahim HY, Elsayed HE, Mohyeldin MM, et al. Norstictic acid inhibits breast cancer cell proliferation, migration, invasion, and in vivo invasive growth through targeting C-Met. *Phyther Res*. 2016;30(4):557–566. doi:10.1002/ptr.5551
27. Sadorn K, Saepua S, Bunbamrung N, et al. Diphenyl ethers and depsidones from the endophytic fungus Aspergillus unguis BCC54176. *Tetrahedron*. 2022;105:132612. doi:10.1016/j.tet.2021.132612
28. Sureram S, Wiyakrutta S, Ngamrojanavanich N, Mahidol C, Ruchirawat S, Kittakoop P. Depsidones, aromatase inhibitors and radical scavenging agents from the marine-derived fungus Aspergillus unguis CRI282-03. *Planta Med*. 2012;78(06):582–588. doi:10.1055/s-0031-1298228
29. Knight T, Luedtke D, Edwards H, Taub JW, Ge Y. A delicate balance – the BCL-2 family and its role in apoptosis, oncogenesis, and cancer therapeutics. *Biochem Pharmacol*. 2019;162:250–261. doi:10.1016/j.bcp.2019.01.015
30. Opferman JT. Attacking cancer's Achilles heel: antagonism of anti-apoptotic BCL-2 family members. *FEBS J*. 2016;283:2661–2675. doi:10.1111/febs.13472
31. Xiao Y, Nimmer P, Sheppard GS, et al. MCL-1 is a key determinant of breast cancer cell survival: validation of MCL-1 dependency utilizing a highly selective small molecule inhibitor. *Mol Cancer Ther*. 2015;14(8):1837–1847. doi:10.1158/1535-7163.MCT-14-0928
32. Vallet S, Fan F, Malvestiti S, et al. Rationally derived drug combinations with the novel Mcl-1 inhibitor EU-5346 in breast cancer. *Breast Cancer Res Treat*. 2019;173:585–596. doi:10.1007/s10549-018-5022-5
33. Williams MM, Lee L, Hicks DJ, et al. Key survival factor, Mcl-1, correlates with sensitivity to combined Bcl-2/Bcl-xL blockade. *Mol Cancer Res*. 2017;15(3):259–268. doi:10.1158/1541-7786.MCR-16-0280-T
34. Nocquet L, Roul J, Lefebvre CC, et al. Low BCL-xL expression in triple-negative breast cancer cells favors chemotherapy efficacy, and this effect is limited by cancer-associated fibroblasts. *Sci Rep*. 2024;14(1):14177. doi:10.1038/s41598-024-64696-z
35. Bertoli C, Skotheim JM, de Bruin RAM. Control of cell cycle transcription during G1 and S phases. *Nat Rev Mol Cell Biol*. 2013;14(8):518–528. doi:10.1038/nrm3629
36. Maddika S, Ande SR, Wiechec E, Hansen LL, Wesselborg S, Los M. Akt-mediated phosphorylation of CDK2 regulates its dual role in cell cycle progression and apoptosis. *J Cell Sci*. 2008;121(7):979–988. doi:10.1242/jcs.009530
37. Mallepogu V, Sankaran KR, Pasala C, et al. Ursolic acid regulates key EMT transcription factors, induces cell cycle arrest and apoptosis in MDA-MB-231 and MCF-7 breast cancer cells, an in-vitro and in silico studies. *J Cell Biochem*. 2023;124(12):1900–1918. doi:10.1002/jcb.30496